

ACTIVE CONTROL OF FAN-GENERATED TONE NOISE

Carl H. Gerhold
 NASA Langley Research Center
 Hampton, Virginia 23681-0001

ABSTRACT

This paper reports on an experiment to control the noise radiated from the inlet of a ducted fan using a time domain active adaptive system. The control sound source consists of loudspeakers arranged in a ring around the fan duct. The error sensor location is in the fan duct. The purpose of this experiment is to demonstrate that the in-duct error sensor reduces the mode spillover in the far field, thereby increasing the efficiency of the control system.

The control system is found to reduce the blade passage frequency tone significantly in the acoustic far field when the mode orders of the noise source and of the control source are the same, when the dominant wave in the duct is a plane wave. The presence of higher order modes in the duct reduces the noise reduction efficiency, particularly near the mode cut-on where the standing wave component is strong, but the control system converges stably.

The control system is stable and converges when the first circumferential mode is generated in the duct. The control system is found to reduce the fan noise in the far field on an arc around the fan inlet by as much as 20 dB with none of the sound amplification associated with mode spillover.

INTRODUCTION

The emergence of the ultra-high bypass ratio engine on aircraft in the 21st century is expected to pose new and significant challenges to the noise control engineers. The dominant engine noise source will shift from the jet to the fan. The blade tip speed will be subsonic or transonic so that the fan noise will have high tonal content at harmonics of the blade passage frequency and the fundamental tone will be at a frequency less than 1000 Hz. In order to provide sufficient thrust, the engine diameter will be on the order of 3.66 meters (12 feet); and, in fact, engine size will be limited by considerations such as space available under the wing and allowable landing gear length. Weight is a significant parameter in the design of the power plant and in order to minimize the weight of the large diameter nacelle, it will be as short and as thin as possible. The relatively low blade passage frequency necessitates thick bulk liner treatment which is extensive in the axial direction, while thickness and length restrictions limit the amount of passive noise control treatment that can be applied.

The conflicting goals of minimum weight and maximum noise reduction can be aided materially by active noise control. Active noise control is well suited for applications in which a low frequency noise source limits the utility of passive control methods.¹ An active noise control system can provide significant noise reduction without excessive weight penalty, and research is continuing on development of light-weight, efficient control sound sources.²

Noise in ducts has long been considered an attractive application of active noise cancellation because the duct serves as a wave guide both to the source noise and to the control sound. Paul Lueg was issued a patent nearly 60 years ago for control of sound in a long duct using a system that consists of a reference microphone to measure the noise to be controlled, a source for the control sound which is equal in

amplitude but opposite in phase with the noise at that point, and a processor that delays to adjust for propagation from the measurement microphone to the control source.³ A major problem has delayed implementation of this control concept and it is the instability that is caused by feedback of the control signal onto the reference microphone. To control this, one research area takes the direction of development of sound sources that are intended to generate sound that propagates in one direction from the control source, thus reducing the feedback.⁴ Another direction is to develop a model of the feedback loop in the digital signal processor and to subtract the synthesized feedback signal from the measured reference signal.⁵ A third method to control the instability is to eliminate feedback altogether by using a non-acoustic reference, such as the signal from a tachometer on an engine operating at steady state.⁶ Utilization of the non-acoustic reference is appropriate when the source noise is periodic, such as is generated by a fan, and when the controller needs only frequency information about the source. The control system described in this paper uses a non-acoustic reference signal from a blade passage sensor on the fan.

Active noise control systems have been shown to reduce multiple harmonic tones of periodic noise generated in a duct by a loudspeaker.⁷ Numerous researchers have demonstrated control of duct-borne sound generated by fans, either multiple pure tones,^{8,9} or broadband fan noise.⁵ The results reported generally show the noise reduction at the error microphone where the cancellation is expected to be quite effective. Researchers at Virginia Polytechnic Institute and State University have developed an active control system on the inlet of a commercial jet engine using a ring of loudspeakers as the control source.¹⁰ The error microphones, which are located in the acoustic far field for the experiments with this engine, have a large diaphragm so that the sound is effectively integrated over a finite space. The result is a broadened spatial extent of noise reduction with a slight loss in magnitude. The most significant problem encountered in this experiment is the mode spillover due to mismatch of the mode compositions of the noise and the control sources. This mode spillover results in noise amplification at some locations away from the control microphones.

The purpose of the experiment reported in the present paper is to develop a control system utilizing error sensors located in the fan duct. It is felt that the spatial extent of noise reduction and, more importantly, the mode spillover effect, can be controlled more effectively with the in-duct error sensor.

CONTROL THEORY

This section discusses the general theoretical development of the Least Mean Square (LMS) Algorithm and the Adaptive Filter. The block diagram of the generalized control system is shown in figure 1. The block labeled "PLANT" indicates a transfer function in which some measurable continuous signal s is the input and the output is a disturbance signal d . The control system signified by the dashed lines generates a discretized signal y_k which combines with the disturbance to produce an error ϵ . It is the purpose of the control system to generate the signal which minimizes the error.

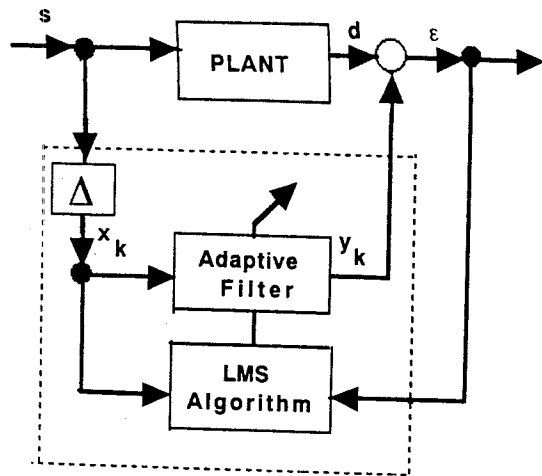


FIGURE 1. Generalized Control System.

The continuous signal, s , is sampled at discrete time intervals, Δ , in the digital computer and collected into a vector X_k of length n :

$$X_k = \begin{Bmatrix} x_k \\ x_{k-1} \\ \vdots \\ \vdots \\ x_{k-n+1} \end{Bmatrix}$$

The element x_k is the digitized sample of s taken at the present time. The element x_{k-1} is the digitized sample of s taken on the previous loop, Δ seconds in the past, and so on to x_{k-n+1} which is the digitized sample of s taken $(n-1)\Delta$ seconds in the past. The vector X_k is constantly updated on each loop with the oldest value discarded, and the newest value put in the top of the array. The scalar output of the adaptive filter is obtained from:

$$(1) \quad y_k = \sum_{l=0}^{n-1} w_l x_{k-l} = W^T X_k$$

where:

W^T = the transpose of the vector W and
 W = a vector of weighting coefficients;

$$W = \begin{Bmatrix} w_0 \\ w_1 \\ \vdots \\ \vdots \\ w_{n-1} \end{Bmatrix}$$

The error at time t_k is the combination of the disturbance and the filter output:

$$(2) \quad \epsilon = d - W^T X_k$$

The mean square error, ϵ^2 , is minimized by setting to zero the derivative of the expectation of the mean square error with respect to the weighting vector.¹¹ The LMS Algorithm is intended to approximate the optimum solution in real time, using the method of steepest descent. The weight function for the current loop through the controller, W_j is updated using the weight function from the previous pass through the loop, W_{j-1} plus a change proportional to the negative gradient of the mean square error, ∇_j

$$(3) \quad \nabla_j = \begin{Bmatrix} \frac{\partial(\epsilon_k^2)}{\partial w_0} \\ \vdots \\ \frac{\partial(\epsilon_k^2)}{\partial w_{n-1}} \end{Bmatrix} = 2 \epsilon_k \begin{Bmatrix} \frac{\partial(\epsilon_k)}{\partial w_0} \\ \vdots \\ \frac{\partial(\epsilon_k)}{\partial w_{n-1}} \end{Bmatrix}$$

where:

ϵ_k = the current value of the digitized sample the error.

The slope of the error curve is evaluated from expression 2:

$$(4) \quad \begin{Bmatrix} \frac{\partial(\epsilon_k)}{\partial w_0} \\ \vdots \\ \frac{\partial(\epsilon_k)}{\partial w_{n-1}} \end{Bmatrix} = X_k$$

The weighting vector is updated in the LMS Algorithm according to the expression:

$$(5) \quad \begin{aligned} W_j &= W_{j-1} - 2 \mu \nabla_j \\ &= W_{j-1} - 2 \mu \epsilon_k X_k \end{aligned}$$

where:

μ = user defined adaptation constant

The algorithm will converge in the mean and will be stable as long as the adaptation constant μ is positive and less than the reciprocal of the largest eigenvalue of the matrix formed from the product of the vector X_k and its transpose.¹¹ The speed with which the algorithm converges is dependent on the adaptation coefficient and the convergence is greatest for the largest value of μ that does not violate the maximum value criterion. The expected value of the weight vector in expression 5 converges to the optimum Weiner weight vector when the input vectors are uncorrelated over time.

MODAL DESCRIPTION OF SOUND PROPAGATION IN DUCTS

The homogeneous wave equation for sound pressure of frequency ω traveling in a cylindrical duct in quiescent air is solved in order to define the natural frequencies and mode shapes:

$$(6) \quad \frac{1}{r} \frac{\partial}{\partial r} \left(r \frac{\partial p}{\partial r} \right) + \frac{1}{r^2} \frac{\partial^2 p}{\partial \theta^2} + \frac{\partial^2 p}{\partial z^2} + k^2 p = 0$$

where:

$$k = \frac{\omega}{c}$$

c = speed of sound

r = the radial coordinate

z = the axial coordinate

θ = the circumferential coordinate

The solution of the wave equation has the general form:

$$(7) \quad p(r, \theta, z) = e^{ik_z z} \{ A_m J_m(k_{mn} r) + i B_m Y_m(k_{mn} r) \} \cos(m\theta)$$

NASA LaRC. The inlet to the fan duct is in the anechoic chamber and the remainder of the duct is in the model assembly area adjacent to the chamber. Figure 2 shows a schematic of the overall experiment layout. The anechoic chamber volume is 482 m³ (17000 ft³) and the acoustic wedges on floor, walls, and ceiling are 0.91 m (3 feet) deep, giving a lower cut-off frequency of approximately 100 Hz. Far field sound measurements are made using a 12.7 mm (1/2 inch) B&K microphone on a rotating boom at a radius of 1.52 m (5 feet) from the face of the duct inlet. An inflow control device is installed on the inlet of the duct.¹⁴ The purpose of the inflow control device is to straighten flow into the duct and to break up turbulent eddies which may be ingested into the fan. The inflow control device is designed to simulate the uniform inflow of forward flight in a static test.¹⁵ Figure 3 is a photograph of the inflow control device on the duct inlet installed in the anechoic chamber. The figure also shows the far field microphone.

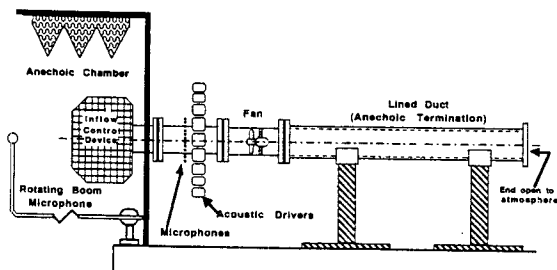


FIGURE 2. Fan noise control experiment layout.

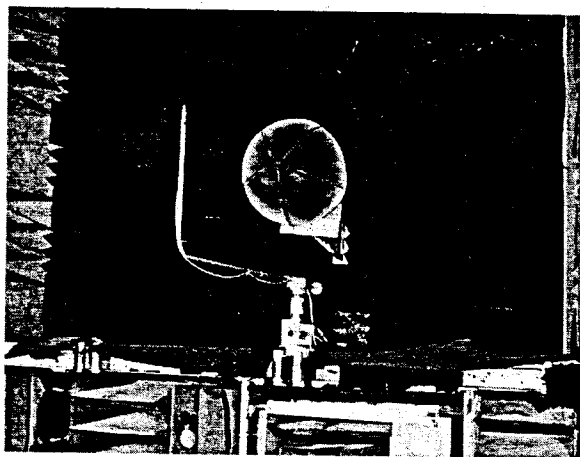


FIGURE 3. Fan noise control ductwork, view from inside the anechoic chamber showing inflow control device and far field microphone.

The control hardware duct piece contains 24 microphones arranged uniformly around the circumference of the duct and installed flush with the inside surface of the duct. The error sensors in the control system are taken from among these 24 microphones. The microphones are 3.2 mm (1/8 inch) diameter transducers embedded in a threaded 12.7 mm (1/2 inch) diameter canister. Twelve control drivers are distributed around the duct, as shown in the photograph, figure 4. Each driver is rated at 120 W rms. The drivers are attached to the duct by transition horns that are thick-walled to prevent sound transmission. The horns transition from the round outlet of the driver to the rectangular slot in the duct wall. The areas of both are the same, so

The circumferential term, $\cos(m\theta)$, satisfies the boundary condition that the sound pressure at angle θ must be the same as the sound pressure at $\theta + 2\pi$. The coefficient m defines the order of the circumferential or spinning mode.

The radial term consists of Bessel functions of the first and second kind. The radial wave numbers, k_{mn} are evaluated from the n zeros of the derivatives of the Bessel functions associated with the m^{th} circumferential mode. The terms come from the boundary condition of zero radial velocity at the duct outer wall and inner hub.

The axial wavenumber is evaluated from the relationship

$$(8) \quad k_z = \sqrt{k^2 - k_{mn}^2}$$

When the sound frequency is high enough that the wavenumber k is greater than the wavenumber of the n^{th} radial mode associated with the m^{th} circumferential mode, k_z is real and sound propagates. The m, n mode is thus said to be cut on. For low frequencies such that $k < k_{mn}$, k_z is imaginary. The argument of the exponential term in equation 7 is real and negative indicating that the sound pressure decays as it moves down the duct. The modes for which $k < k_{mn}$ are said to be cut off.

The plane wave is always present in the duct since it cuts on at 0 Hz. The first two spinning modes corresponding to the lowest order radial mode cut on at wave number normalized by the outer radius of the duct, $ka=1.84$ for the (1,0) mode and $ka=3.05$ for the (2,0) mode.¹² The zero order spinning mode associated with the first radial mode (0,1) cuts on at $ka=3.83$. These are the values expected for a duct with no centerbody.

The tonal part of the fan noise is generated by the impingement of the vortices shed from the rotor on the downstream fan exit guide vanes. These tones occur at the blade passage frequency and its harmonics. When the frequency is high enough that the wave can propagate, the fan tones travel in spinning modes defined from the relationship:¹²

$$(9) \quad m = n_h B + kV$$

where:

- n_h = harmonic number
- B = number of blades
- V = number of fan exit guide vanes
- k = any positive or negative integer, including zero

When the number of blades and the number of vanes is the same, the plane wave, $m=0$, is most strongly excited. When the difference in the number of blades and vanes is 1, the first spinning mode will dominate at frequencies above the $m=1$ cut-on. The spinning mode is characterized by a sound radiation deficit on the fan axis. The sound is in a lobe which radiates perpendicular to the duct axis when the mode is first cut on and progresses toward the duct axis as the frequency increases.¹³

EXPERIMENT LAYOUT

Duct

The experimental setup consists of a duct with the following major elements: inflow control device, control hardware section, an axial flow fan, and an anechoic termination. The unit is installed in the laboratory space of the Anechoic Noise Facility at

Figure 6 shows the directivity plot of fan noise in the acoustic far field with the fan operating at 2350 rpm. The blade passage frequency at this fan speed is 627 Hz, and the normalized wavenumber, ka , is 1.76. The blade passage frequency is thus below the first spinning mode cut-on, and it is expected that only plane waves will propagate in the duct. The microphone signal has been filtered so that the directivity plot in figure 6 shows the blade passage frequency tone. When the controller is not activated, the directivity plot shows sound radiation that is spatially uniform, confirming the expected plane wave sound propagation in the duct. When the controller is activated, the curves in the figure indicate that the sound level is reduced approximately 14 dB in the far field for observer locations from 0° to 90° . This noise reduction was found to be quite stable throughout the time that it took to complete the directivity sweep.

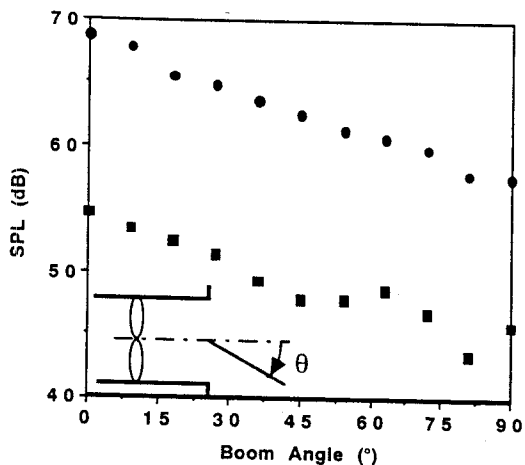


FIGURE 6. Far field directivity of BPF tone at fan speed 2350 rpm, plane wave dominant.
● : control off, ■ : control on

The fan was then run at 2800 rpm, which corresponds to blade passage frequency of 750 Hz or normalized wavenumber $ka=2.10$. This frequency is above the first spinning mode cut-on frequency for the duct, but it is expected that the spinning mode would not be cut on strongly in light of the fact that the number of blades and stators is the same. This is seen in the directivity plots of the blade passage frequency tones for control off and control on that are shown in figure 7. The far field sound is not as uniform spatially as it was below the mode cut-on, figure 6, indicating the presence of a higher order mode. However, the sound deficit on the fan axis that is characteristic of the spinning mode dominance is not found in the radiation pattern in figure 7, which indicates plane wave dominance. When the controller is activated, the sound level reduction is relatively uniform at 2 dB in the acoustic far field at locations from the fan axis to 90° . The far field noise reduction, while stable and spatially uniform, is much less than it is when blade passage frequency is below the spinning mode cut-on.

The performance of the controller as a function of frequency is indicated in figure 8. This plot was generated by operating the fan at speeds from 1500 rpm to 6000 rpm and comparing the blade passage frequency tones at the error microphone for control off with control on at each speed. The control off spectrum for the in-duct error microphone shows a general trend in sound level to go up with engine speed punctuated by increases at 2300, 3700, and 4900 rpm. The increases indicate the presence of standing waves in the duct. The 2300 rpm speed is

near the cut-on of the first spinning mode. The sound level increase at this frequency is not large because the generation mechanism for the higher order spinning modes is weak. The cause of the increases in sound level at 3700 and 4800 rpm as indicated in figure 8 are not known at this time since these speeds are significantly below the second spinning and lowest radial mode cut-on. When the controller is activated, the system reaches steady state with the error microphone signal decreased at all operating speeds. The noise reduction is from 3 dB to as much as 27 dB at the error microphone.

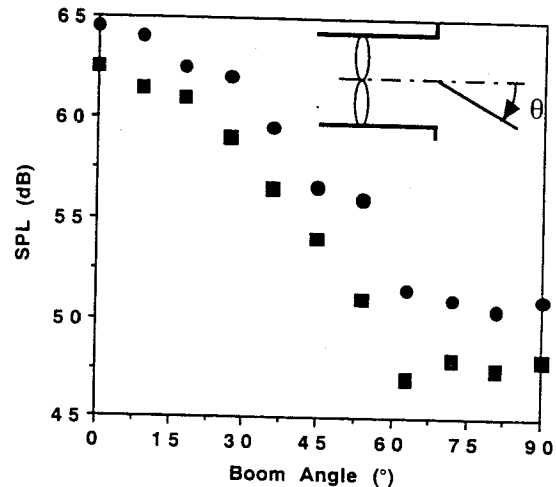


FIGURE 7. Far field directivity of BPF tone at fan speed 2800 rpm, plane wave dominant.
● : control off, ■ : control on

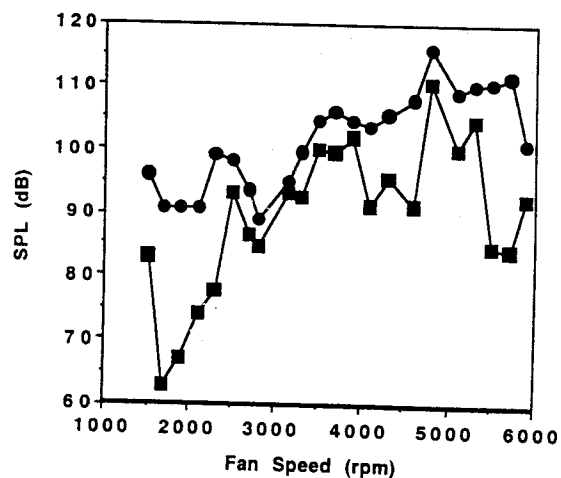


FIGURE 8. Sound level spectrum of fan BPF tone at in-duct error microphone.
● : control off, ■ : control on

Figure 9 shows the spectral noise reduction achieved in the far field on the axis of the duct. When the control is off, the far field spectrum is smoother than it is in the duct, showing that the duct standing waves are not propagated into the far field. Noise reduction is obtained with the controller at all operating speeds except 2700, 3900, and 5700 rpm. These critical fan speeds are near those at which the in duct error microphones registered standing waves in the duct. Comparison of figures 8 and 9 show that the noise reduction in the far field is generally less

than that indicated by the in-duct error microphones. In fact the error microphone signal indicated noise reduction at the critical speeds and the sound level in the far field was either not affected or was increased.

2. Spinning Mode Generated in the Duct

A test series was run in which 17 fan exit guide vanes are installed into the fan duct, while the rotor blade count of 16 is retained. It is expected that the difference in the number of vanes and rotor blades will cause the $m=1$ spinning mode to be excited. The output from two microphones mounted on opposite circumferential locations in the duct are added out-of-phase to give the error signal. The phase of the signal to each of the 12 control loudspeakers is shifted by 30° relative to the previous driver in order to simulate the $m=1$ mode.

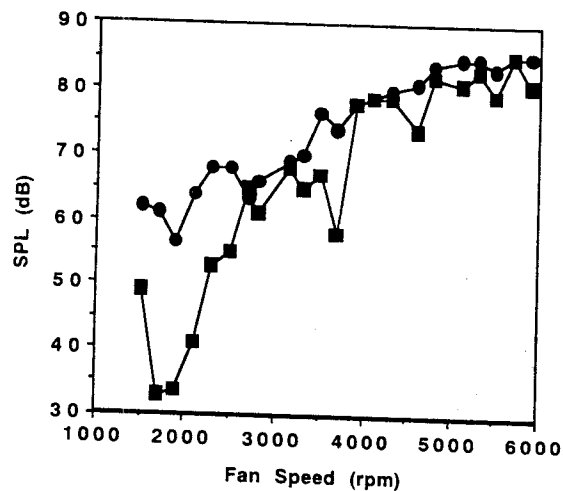


FIGURE 9. Sound level spectrum of fan BPF tone at far field microphone fixed on the duct axis, $\theta = 0^\circ$.
● : control off, ■ : control on

The fan was operated at 2800 rpm, which speed produces normalized wavenumber $ka = 2.10$. This is above the first spinning mode cut-on and it is expected that the $m=1$ spinning mode will be excited into dominance. This is shown in the far field radiation pattern, the lower curve in figure 10. The upper curve in figure 10 shows directivity of the experimental simulation produced by the control drivers at 750 Hz. The far field radiation pattern generated by the control drivers is seen to be comparable to the fan noise radiation.

The result of activating the control system is shown in figure 11. The spinning mode is virtually eliminated, leaving a radiation pattern that suggests a plane wave. This is reasonable since the plane wave is always generated by the fan and the control system is not programmed to reduce it.

CONCLUSIONS

The experiments discussed in this paper have verified that time domain active, adaptive control is applicable to reduction of fan noise in a duct. The control system has been applied to tones that are generated at the blade passage frequency. The controller is stable over a range of frequencies in which plane waves and higher order duct modes can propagate. The system utilizes in-duct error sensing which is shown to provide global noise reduction in the acoustic far field.

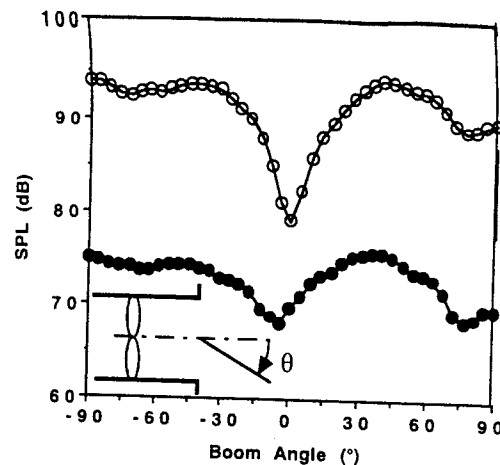


FIGURE 10. Comparison of fan BPF tone to simulation in the far field, fan speed at 2800 rpm, $m=1$ mode dominant
○ : simulation, ● : fan tone.

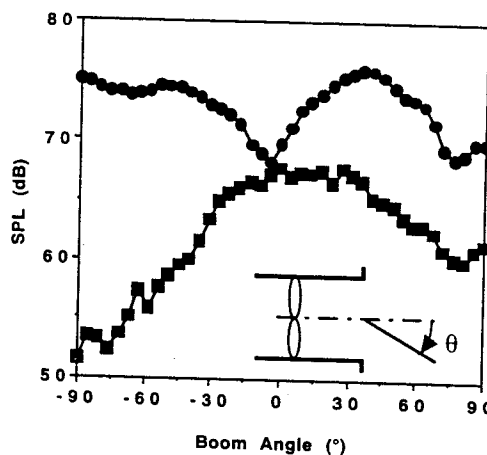


FIGURE 11. Far field directivity of BPF tone at fan speed 2800 rpm, $m=1$ mode dominant.
● : control off, ■ : control on

The system is most effective when the mode structures of the noise source and of the control source are the same. When the fan is configured with equal numbers of rotor blades and stator vanes, and the control drivers are configured to generate plane waves, far field noise reduction is greatest below cut-on of higher order modes. The presence of higher order modes, even though the plane wave is dominant, compromises noise reduction performance. When the number of stator vanes and rotor blades differs by 1, and the control drivers are programmed to generate the $m=1$ mode, the control system reduces the first spinning mode, leaving the plane wave component which is inevitably generated by the rotor/stator interaction. The in-duct error sensor produces a stable control signal which does not excite uncontrolled higher order modes.

Generally the noise reduction measured by the in-duct error sensors is greater than the noise reduction in the far field. Fan operating conditions were found at which the in-duct error sensor indicated noise reduction but no noise reduction was measured in the far field. In some instances the sound in the far field was increased with the control system activated, even

though the control system stabilized at significant noise reduction at the error microphone. These conditions occurred when standing waves were present in the duct. This condition is felt to be due to the fact that the control system is reducing the (dominant) standing wave component of the sound while not affecting the propagating component. The discrepancy between the in-duct error sensor performance indication and the far field noise reduction is the subject of continued research.

REFERENCES

1. Chaplin, G.B., 1983, "Anti-Noise, the Essex Breakthrough", *Chartered Mechanical Engineer*, vol. 30, pp. 41-47.
2. Dungan, M.E., 1992, "Development of a Compact Sound Source for the Active Control of Turbofan Inlet Noise", MS Thesis, Virginia Polytechnic Institute and State University, Blacksburg, Virginia.
3. Lueg, P., 1936, "Process of Silencing Sound Oscillations", U.S. Patent number 2,043,416.
4. Swinbanks, M.A., 1973, "The Active Control of Sound Propagation in Long Ducts", *Journal of Sound and Vibration*, vol. 27, pp. 411-436.
5. Eriksson, L.J., Allie, M.C., Bremigan, C.D., and Gilbert, 1989, J.A., "Active Noise Control on Systems with Time-Varying Sources and Parameters", *Sound and Vibration*, vol. 23, no. 7, pp. 16-21.
6. Eghtesadi, K. and Chaplin, G.B., 1987, "The Cancellation of Repetitive Noise and Vibration by Active Methods", proceedings of NOISE-CON '87, State College, Pennsylvania, pp. 347-352.
7. Tichy, J., Warnacha, G.E., and Pool, L.A., 1984, "Active Noise Reduction Systems in Ducts", ASME paper no. 84-WA/NCA-15.
8. Ffowcs Williams, J.E., 1981, "The Silent Noise of a Gas Turbine", *Spectrum, British Science News*, vol. 175, no. 1.
9. Koopman, G.H., Fox, D.J., and Niese, W., 1988, "Active Source Cancellation of the Blade Tone Fundamental and Harmonics in Centrifugal Fans", *Journal of Sound and Vibration*, vol. 126, pp. 209-220.
10. Thomas, R.H., Burdisso, R.A., Fuller, C.R., and O'Brien, W.F., 1993, "Active Control of Fan Noise from a Turbofan Engine", AIAA paper no. 93-0597.
11. Widrow, B., Glover, J.R., McCool, J.M., Kaunitz, J., Williams, C.S., Hearn, R.H., Zeidler, J.R., Dong, E., and Goodlin, R.C., 1975, "Adaptive Noise Canceling: Principles and Applications", *Proceedings of the IEEE*, vol. 63, no. 12, pp. 1692-1716.
12. Tyler, J.M. and Sofrin, T.G., 1962, "Axial Flow Compressor Noise Studies", *SAE Transactions*, vol. 70, pp. 309-332.
13. Rice, E.J., 1978, "Multimodal Far-field Acoustic Radiation Using Mode Cutoff Ratio", *AIAA Journal*, vol. 16, pp. 906-911.
14. Homyak, L., McArdle, J.G., and Heidelberg, L.J., 1983, "A Compact Inflow Control Device for Simulating Flight Fan Noise", AIAA paper no. 83-0680.
15. Chestnutt, D. ed., 1982, "Flight Effects of Fan Noise", NASA CP-2242.